Thermal and Electrooptical Properties of Ferroelectric Liquid Crystals Having OH Groups

Kazuo SUGIYAMA,* Koichi KATO, and Kohei SHIRAISHI
Department of Industrial Chemistry, Faculty of Engineering, Kinki University, Hirokoshinkai, Kure, Hiroshima 737-01
(Received November 13, 1990)

Four kinds of ferroelectric liquid crystals (FLCs) possessing OH groups, ((*S*)-2-methylbutyl 4-[4-(11-hydroxyundecyloxy)benzylideneamino]cinnamate **4a**, (*S*)-2-methylbutyl 4-[4-(11-hydroxyundecyloxy)-2-hydroxybenzylideneamino]cinnamate **4b**, (*S*)-2-hydroxypropyl 4-[4-(11-hydroxyundecyloxy)benzylideneamino]cinnamate **4c**, and (*S*)-2-hydroxypropyl 4-[4-(11-hydroxyundecyloxy)-2-hydroxybenzylideneamino]cinnamate **4d**) were prepared in order to understand how the introduction of OH groups in FLCs affect the phase behavior and electrooptical effects. α,ω-Diols **4c** and **4d** show a higher transition temperature of the smectic A (S_A) phase than do ω-hydroxyl compounds **4a** and **4b**. Comparing **4b** and **4d** both of which have an OH group at the *o*-position of the benzylidene group with **4a** and **4c**, the former samples show a higher S_A-isotropization (I) transition temperature than do the latter ones. It is suggested from IR spectroscopic results that inter- and intramolecular hydrogen bonding contribute to the stabilization of the S_A phase. The order of the helical pitch in the chiral smectic C (S_c*) phase was found to be **4b**>**4a**>**4d**>**4c** within 1.8—6.6 μm. From an electrooptical effect due to a deformation of the helical structure in the S_c phase, the rise time of the surface director (τ_{sr}) and the rise time of the bulk director (τ_{br}) were measured to be as follows: τ_{sr} are 850, 1500, 30, and 70 μs, and τ_{br} are 12, 100, 0.17, and 0.35 ms for **4a**, **4b**, **4c**, and **4d**, respectively. It was found that the intramolecular hydrogen bonding results in a slower optical response time, whereas intermolecular hydrogen bonding results in a faster one.

Since the discovery of a ferroelectric property in the S_c* phase by Meyer et al.,[1] (*S*)-2-methylbutyl-4-[4-(decyloxy)benzylideneamino]cinnamate (DOBAMBC) has attracted much attention regarding both fundamental physical science[2-5] and practical view points concerning various types of electrooptical materials with small switching times and memory effects.[6-10] Many scientific and practical efforts have also been concentrated on families of FLCs, such as chiral compounds with benzylideneaniline,[11-13] biphenyl,[14,15] phenylbenzoate[16-18] used as mesogenic units. On the other hand, ferroelectric liquid crystalline polymers (FLCPs) that combine the mechanical properties of polymeric material and the physical properties of FLCs have also been an active, growing area of research interest for many years. FLCPs have been achieved in various polymers having chiral mesogens as a pendant group on the main chain such as polysiloxane,[19,20] polyvinyl[21-23] and polyester backbones.[24-26] Few FLCPs having chiral mesogenic groups as blocks within the main chain are presently known.[27] In previous papers[28-30] we have reported on the properties of terminal-terminal-type FLCs as twin models for the main-chain-type of FLCs which contain mesogenic units interconnected through spacer groups. As a part of an ongoing study of FLCPs, we have prepared novel DOBAMBC analogous with the structures designated **4a**—**4d** in scheme 1. α,ω-FLC diols **4c**, **4d** can be used as mesogenic units in FLCPs with various structures such as polyurethane, polyester, and polycarbonate. In the present study differential scanning calorimetry (DSC) and polarized optical microscopy (POM) were applied to an investigation of the thermal behavior of FLCs, also two types of electrooptical effects, such as a surface-stabilized FLC (SSFLC) cell and a transient scattering mode (TMS) device, were measured for possible applications.

Experimental

Syntheses: Novel types of FLCs **4a**—**4d** were prepared using the following route, as shown in Scheme 1.

4-(11-Hydroxyundecyloxy)benzaldehydes **1**; Aldehyde **1a** and **1b** were obtained from a reaction of 4-hydroxybenzaldehyde or 2,4-dihydroxybenzaldehyde and 11-bromoundecanol in the presence of K_2CO_3 and KI, according to the method of Ringsdorf et al.[31]

4-(11-Hydroxyundecyloxy)benzaldehyde **1a**: 80.5% yield; mp 61—62 °C; ^{1}H NMR ($CDCl_3$) δ=1.12—2.28 (m, 18H), 3.72—3.92 (t, 2H), 4.20—4.44 (t, 2H), 8.32—8.48 (q, 4H), and 10.05 (s, 1H). Found: C, 73.82; H, 9.48%. Calcd for $C_{18}H_{28}O_3$ (M, 292.422): C, 73.93; H, 9.65%.

2-Hydroxy-4-(11-hydroxyundecyloxy)benzaldehyde **1b**: 57.3% yield; mp 56—58 °C; ^{1}H NMR ($CDCl_3$) δ=1.06—2.09 (m, 18H), 3.33—3.69 (t, 2H), 3.81—4.03 (t, 2H), 6.22—7.37 (q, 3H), and 9.18 (s, 1H). Found: C, 70.05; H, 9.02%. Calcd for $C_{18}H_{28}O_4$ (M, 308.421): C, 70.10; H, 9.15%.

(*S*)-2-Hydroxypropyl 4-nitrocinnamate **2a**: To 0.2 mol (*S*)-1,2-propanediol and 50 mL pyridine in 300 mL freshly distilled THF, 0.16 mol 4-nitrocinnamoyl chloride in 100 mL THF was added with stirring at 0 °C for 2 h. After stirring for an additional 10 h at room temperature, the reaction mixture was evaporated to dryness, and ca. 300 mL of chloroform was added to the residue. The chloroform layer was washed with water and evaporated to dryness. The obtained product was recrystallized from methanol to give yellow crystals: 73.3% yield; mp 72—74 °C; ^{1}H NMR ($CDCl_3$) δ=1.12—1.52 (m, 3H), 3.28—3.64 (m, 1H), 4.04—4.60 (m, 2H), 6.60—6.80 (d, J=16 Hz, 1H), and 7.60—8.48 (q, 5H). Found: C, 57.41; H, 5.25; N, 5.34%. Calcd for $C_{12}H_{13}NO_5$ (M, 251.241): C, 57.37; H, 5.22; N, 5.58%.

(*S*)-2-Hydroxypropyl 4-aminocinnamate **3a**: To 0.04 mol **2a** and 0.84 mol $FeCl_2$ in 300 mL methanol, gaseous NH_3 was gently introduced with stirring at room temperature for 1.5 h.

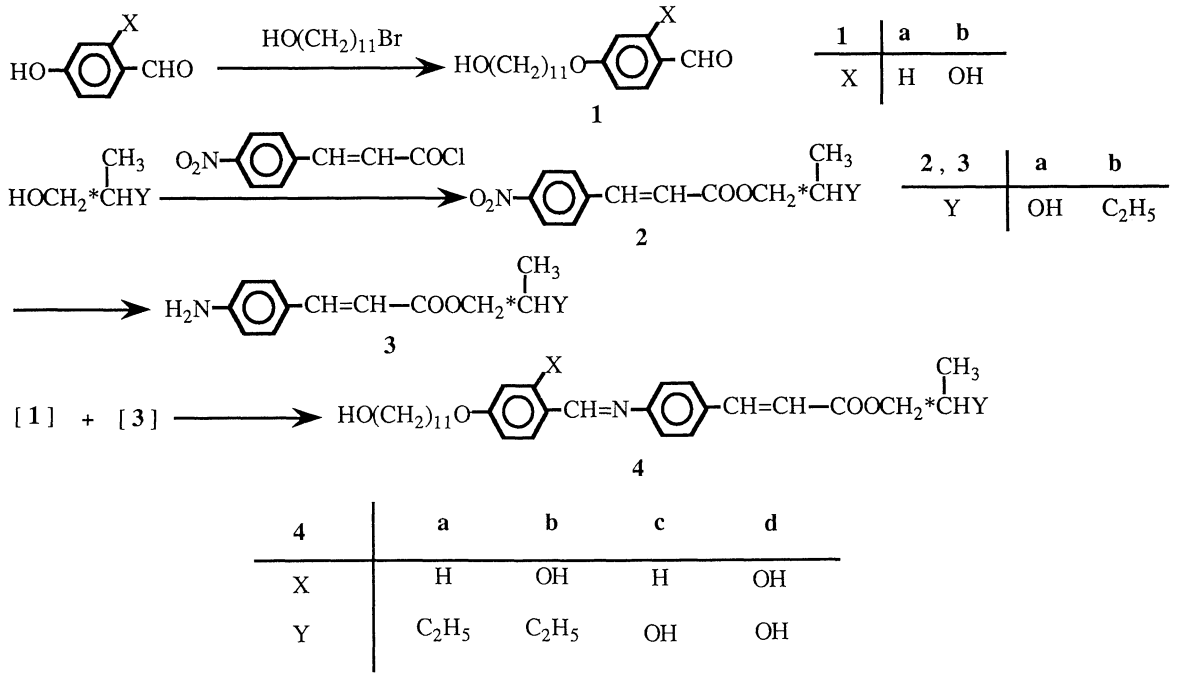

1	a	b
X	H	OH

2, 3	a	b
Y	OH	C_2H_5

4	a	b	c	d
X	H	OH	H	OH
Y	C_2H_5	C_2H_5	OH	OH

Scheme 1. Preparation of ferroelectric liquid crystalline α,ω-diols.

Table 1. NMR Spectra and Elemental Analysis of **4**

4	^{1}H NMR ($CDCl_3$)	Elemental analysis/%			Phase transition temperature	$\Delta T_{S_C^*}$	ΔT_{S_A}
	δ/ppm	C	H	N	°C	°C	°C
4a	0.80—1.08 (m, 6H), 1.14—2.00 (m, 21H), 3.50—3.72 (t, 2H), 3.84—4.24 (m, 4H), 6.18—6.48 (d, J=16 Hz, 1H), 6.80—7.88 (m, 9H), 8.30 (s, 1H)	$C_{32}H_{45}O_4N$=507.720			K 68 S_C* 91 S_A 109 I	23	18
		Found 75.46	9.06	2.61			
		Calc. 75.70	8.93	2.76			
4b	0.74—1.07 (m, 6H), 1.12—1.96 (m, 21H), 3.43—3.71 (t, 2H), 3.78—4.18 (m, 4H) 6.26—6.36 (d, J=16 Hz, 1H), 7.34—7.64 (m, 8H), 8.43 (s, 1H)	$C_{32}H_{45}O_5N$=523.719			K 62 S_C* 86 S_A 120 I	24	34
		Found 73.84	8.55	2.58			
		Calc. 73.99	8.66	2.67			
4c	0.80—1.56 (m, 18H), 1.60—1.90 (m, 3H), 3.28—3.56 (t, 3H), 3.68—4.08 (m, 4H) 6.16—6.44 (d, J=16 Hz, 1H), 6.68—7.76 (m, 9H), 8.22 (s, 1H)	$C_{30}H_{41}O_4N$=496.665			K 57 S_H* 112 S_C* 132 S_A 147 I	20	15
		Found 72.60	8.32	2.60			
		Calc. 72.70	8.34	2.83			
4d	0.90—1.56 (m, 18H), 1.62—1.92 (m, 3H), 3.34—3.58 (t, 3H), 3.68—4.12 (m, 4H), 6.20—6.48 (d, J=16 Hz, 1H), 7.00—7.66 (m, 9H), 8.46 (s, 1H)	$C_{30}H_{41}O_5N$=511.664			K 67 S_C* 107 S_A 155 I	40	48
		Found 70.38	8.15	2.61			
		Calc. 70.42	8.08	2.74			

After reduction was completed, the reaction mixture was evaporated to dryness. The residue was extracted three times with 100 mL of dichloromethane. The dichloromethane layer was washed with water and evaporated to dryness. The obtained product was chromatographed on silica gel (Wakogel C-200) with diethyl ether to give yellow crystals; 74.8% yield; mp 83—84 °C; ^{1}H NMR ($CDCl_3$) δ=1.04—1.44 (m, 3H), 3.26—3.84 (m, 1H), 4.04—4.40 (m, 2H), 6.28—6.44 (d, J=16 Hz, 1H), 6.60—7.82 (m, 5H). Found: C, 64.93; H, 6.71; N, 6.10%. Calcd for $C_{12}H_{15}NO_3$ (M, 221.258): C, 65.14; H, 6.83; N, 6.33%.

Shiff Bases 4: An equimolar mixture of aldehyde **1** and 4-aminocinnamate **3** in 10 mL of absolute ethanol was allowed to stand for 24 h. The precipitate was filtered and recrystallized twice from the absolute ethanol; the yield was ca. 90%. The thermal behaviors and characterization of (*S*)-2-methylbutyl 4-[4-(11-hydroxyundecyloxy)benzylideneamino]-cinnamate **4a**, (*S*)-2-methylbutyl 4-[4-(11-hydroxyundecyloxy)-2-hydroxybenzylideneamino]cinnamate **4b**, (*S*)-2-hydroxypropyl 4-[4-(11-hydroxyundecyloxy)benzylideneamino]cinnamate **4c**, and (*S*)-2-hydroxypropyl 4-[4-(11-hydroxyundecyloxy) 2-hydroxybenzylideneamino]cinnamate **4d** are tabulated in Table 1.

Measurements: ^{1}H NMR measurements were carried out with a 100 MHz JEOL JNM-MH 100 spectrometer. The

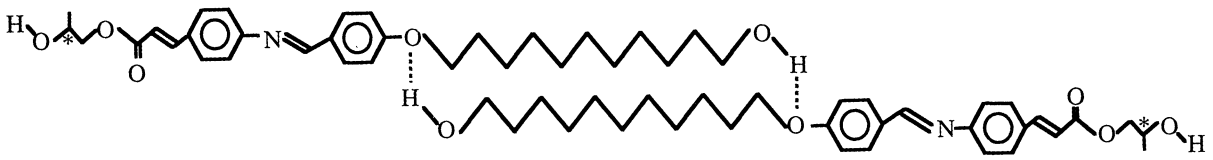

Fig. 1. Structure of intermolecular hydrogen bonds of **4c**.

phase-transition temperature was determined by DSC using a Rigaku Thermoflex apparatus (DSC-8230B). Sample quantities varied from 5 to 10 mg. POM was performed using an Olympus nicroscope (BH-2), with a heating stage attached to a temperature controller. Thin samples were sandwiched between two glass slides, the surfaces of which had been unidirectionally rubbed with cotton wool to obtain a homogeneous alignment. The spacing between the top and bottom glass plates was 25 μm, with a stretched polyester film used as the spacer material. Electrooptical measurements were carried out as follows. The surfaces of glass plates were coated with a transparent conductive material (In_2O_3); the surface resistance was about 100 Ω m^{-2}. The sample cell (thickness: 25 μm) was set without a polarizer in the optical path of a He–Ne laser (NEC-GLG, 5313, wavelength 632.8 nm, and output power 1 mW). The incident light was damped with an attenuator and arranged with a slit. Changes in the transmission upon the application of an electric field were monitored with a photodiode, and processed with a personalcomputer (NEC 9801).

Results and Discussion

Thermal Properties. According to DSC and POM, samples **4a**—**4d** show two or more mesophases upon cooling; at the transition from the I to the S_A phase, a fan-shaped texture with the focal conic texture first appears. Upon further cooling, the S_A phase and the following S_c* phase result, showing a focal conic texture with stripes due to a helical structure.

The phase-transition temperature of a samples determined using DSC is compatible with that obtained by means of POM and the electro-optical measurements mentioned below. The results are summarized in Table 1. From the obtained results it was found that although these samples resemble typical FLC, DOBAMBC (S_H 63 S_c* 95 S_A 118 I) very closely in mesomorphic behavior, their phase-transition temperature is somewhat higher than that of DOBAMBC, itself. The OH stretch vibrations of **4c** and **4d** are broad bands centered at 3425 and 3340 cm^{-1} due to intermolecular hydrogen bonds in the crystalline phase (K), respectively.

It is, thus, suggested that in FLC α,ω-diols **4c** and **4d** hydrogen bonds exist between the hydroxyl hydrogen and the phenyl ether oxygens, as described regarding 4,4′-bis(6-hydroxyhexyloxy)biphenyl.[32] The structure of hydrogen bonding in **4c** is speculated to be as shown in Figure 1. Comparing the thermal behavior of **4b** and **4d** with that of the corresponding liquid crystals, **4a** and **4c**, the former samples show a wider temperature range of both the S_A phase (ΔT_{S_A}) and the S_c* phase (ΔT_{S_c*}) than do that of latter ones. In addition, the phase-transition temperatures of the S_A-I transition of **4b** and **4d** was higher than those of **4a** and **4c**. These results can be explained as follows: the thermal stability of the smectic state in liquid crystals having an OH group at the *o*-position of the benzylidene group, such as in **4b** and **4d**, is increased by an interaction between adjacent molecules in the smectic layers when the hydroxyl hydrogen is intramolecular hydrogen-bonded to give a cis conformation with a narrow molecular breadth and a coplanarity of the two benzene rings.[12,33]

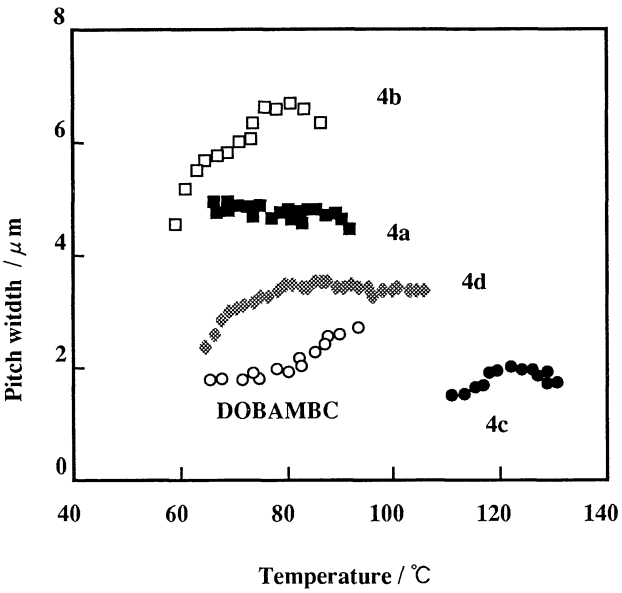

Fig. 2. Temperature dependence of pitch width of helical structure in the S_c* phase of α,ω-diols **4** and DOBAMBC.

The pitches of the helical structure of the S_c* phase, which are important factors concerning the electrooptical effect in FLCs, were measured by averaging the spacing of the stripes at ten different places in a micrograph of their textures. Figure 2 shows the temperature dependence of the pitch of the helical structure in the S_c* phase. The order of the average pitch of the samples was found to be as follows:

4b>4a>4d>4c.

FLC α,ω-diols (**4d** and **4c**) show a narrower pitch than do the others (**4b** and **4a**), while intramolecular hydrogen bonded **4b** and **4d** show a wider pitch than do **4a** and **4c**. This result may be explained in terms of the

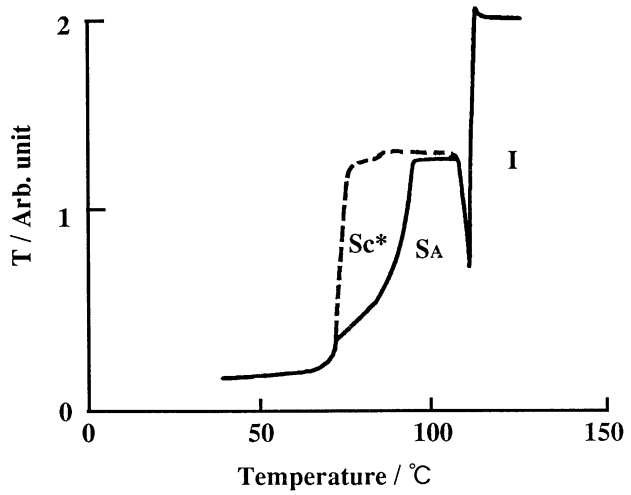

Fig. 3. Transmission intensity (T) of **4a** on cooling cycles: (——); E=0, (-----); E=16 kV cm^{-1}.

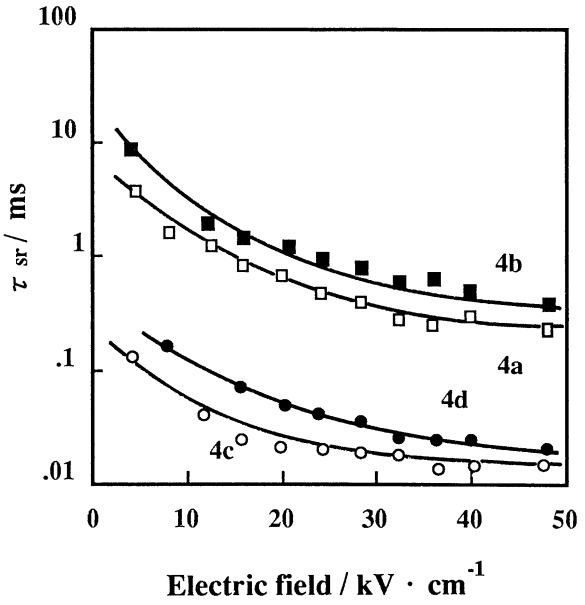

Fig. 4. Electric field dependence of the rise time of surface director (τ_{sr}) in the ferroelectric S_c* phase α,ω-diols **4**.

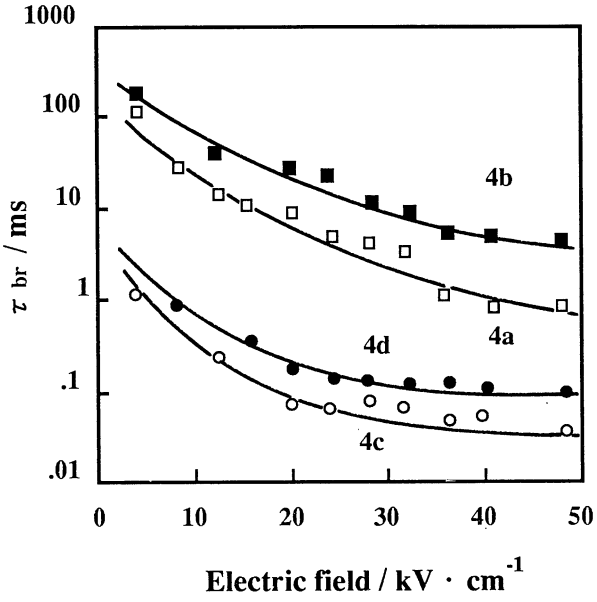

Fig. 5. Electric field dependence of the rise time of bulk director (τ_{br}) in the ferroelectric S_c* phase α,ω-diols **4**.

layer spacing in a smectic phase, depending on the hydrogen bonds between the molecular layers.

Electrooptical Properties. FLC α,ω-diols were measured regarding electrooptical effects in order to obtain basic data for practical uses of FLCs. Figure 3 shows the transmission intensity (T) of the He–Ne laser through the **4a** cell upon cooling. When no voltage was applied, T below 91 °C gradually decreased due to light scattering in the wound phase of the helical structure of the S_c* phase. On the other hand, upon application of a d.c. electric field, T never decreased within the temperature range of the S_c* phase. In this measurement, it was found that T decreases slightly just after a d.c. field application, and then increases remarkably. The applied field induces a fluctuation of the boundary due to a reorientation of the molecular alignment in the layer near to the electrode surface resulting in a decrease of T within a short time (τ_{sr}). This electrooptical effect can be regarded as being a response time of a surface-stabilized ferroelectric liquid crystal (SSFLC) cell.[10] On the other hand, the main response (τ_{br}) corresponding to an increase in T is relatively slow. The slow response, called the transient scattering mode (TSM) effect,[34] is believed to be due to a transformation of a wound phase (S_c*) to unwound phase (S_c): that is, a transition from a helical structure to a uniform monodomain structure. The electrooptical response time corresponding to the change in T caused by a d.c. field application was measured over an electric field from 0.4 to 48 kV cm^{-1} at T_{Sc*} −10 °C (cell thickness; 25 μm). τ_{sr} and τ_{br} are the times taken to reach the stage of a T decrease and increase of up to 90%, respectively. In order to determine the effect of the applied field on the response times, τ_{sr} and τ_{br} were used to measure the S_c* phase by changing the applied voltage. Figures 4 and 5 show the field dependence of the response time in the **4** cell. These figures show that an increase in the applied voltage results in a faster optical response time; an increase in the pitch of helical structure results in a slower response. It was also found by comparing the **4b** and **4d** existing intramolecular hydrogen bonding with **4a** and **4c**, the former samples show a slower optical response time than do the latter ones. In addition, the optical response times of α,ω-FLC diols **4c** and **4d** are faster than that of ω-hydroxyl FLCs **4a** and **4b**. For development of the S_c* phase, it is well known that intermolecular interactions are limited to

Table 2. Thermal and Electrooptical Properties of 4[a)]

4	$T_{S_A\text{-}S_c^*}$ / °C	$T_{S_c^*\text{—}K}$ / °C	Pitch / μm	τ_{sr}[b)] / μs	τ_{br}[b)] / ms
4a	91	23	4.7 (76°C)	850 (76°C)	12 (76°C)
4b	86	24	6.6 (75°C)	1500 (75°C)	100 (75°C)
4c	132	20	1.8 (114°C)	30 (114°C)	0.17 (114°C)
4d	107	40	3.5 (89°C)	70 (89°C)	0.35 (89°C)
DOBAMBC	95	33	1.7 (90°C)	200 (90°C)	120 (75°C)

a) Cell thickness; 25 μm. b) Electric field=16 kV cm^{-1}.

excluded volume effects and dispersive forces. In our case, in addition to the interaction due to these two factors, hydrogen bonding plays an important role in the formation of the S_c^* phase and in the optical response time corresponding to a change in the helical structure in the S_c^* phase. So far, the relationship between the pitch and the response time in our samples is not explicable, since it is not at all clear how large their spontaneous polarization (P_s) and viscosity (η) are. An explanation for this observed interesting relationship will be provided when the P_s and η are measured. The optical response times at 16 kV cm^{-1} are summarized in Table 2. Since the samples obtained as new types of FLCs show a relatively high-speed electrooptical effect with a low-threshold field of less than 5 kV cm^{-1}, these samples can be practically applied as display devices.

From the results concerning the thermal and electrooptical characterization of DOBAMBC analogous FLCs **4a**—**4d**, the following conclusions can be drawn:

1. α,ω-Diols **4c** and **4d** show a higher transition temperature of S_A phase than do ω-hydroxyl compounds **4a** and **4b**. Since α,ω-diols **4c** and **4d** also exhibit a higher S_A transition temperature than does DOBAMBC, the introduction of OH as terminal groups was found to stabilize the S_A phase, based on intermolecular hydrogen bonding.

2. Comparing **4b** and **4d** having an OH group at the *o*-position of the benzylidene group with **4a** and **4c**, the former samples show a higher transition temperature of S_A–I than do the latter ones. It is suggested that intramolecular hydrogen bonding contributes to a stabilization of the S_A phase.

3. Intramolecular hydrogen bonding results in a wider helical pitch, while the intermolecular hydrogen bonding results in a narrower one.

4. From the electrooptical measurements, it was found that a wider helical pitch results in a slower optical response time.

5. The τ_{sr} for SSFLC of **4a**—**d** is slower than that of DOBAMBC, whereas the τ_{br} for TSM is faster than that of DOBAMBC.

References

1) R. B. Meyer, L. Liebert, L. Strzelecki, and P. Keller, *J. Phys. Lett.*, **36**, L-69 (1975).
2) N. Maruyama, *Ferroelectrics*, **63**, 49 (1985).
3) S. Kai, T. Hashimoto, M. Nomiyama, and M. Imasaki, *Jpn. J. Appl. Phys., Suppl.*, **24**, 890 (1985).
4) H. Takezoe, Y. Ouchi, K. Ishikawa, and A. Fukuda, *Mol. Cryst. Liq. Cryst.*, **139**, 27 (1986).
5) K. Kondo, S. Era, M. Isogai, and A. Mukoh, *Jpn. J. Appl. Phys.*, **24**, 1389 (1985).
6) J. S. Patel, *Appl. Phys. Lett.*, **47**, 1277 (1985).
7) M. Ozaki, S. Kishio, Y. Shigeno, and K. Yoshino, *Jpn. J. Appl. Phys., Suppl.*, **24**, 63 (1985).
8) K. Yoshino, M. Ozaki, T. Sakurai, and M. Honma, *Jpn. J. Appl. Phys., Suppl.*, **24**, 59(1985).
9) K. Yoshino, S. Kishio, M. Ozaki, T. Sakurai, N. Mikami, and R. Higuchi, *Jpn. J. Appl. Phys.*, **25**, L976 (1986).
10) S. Kishio, M. Ozaki, K. Yoshino, and A. Sakamoto, *Mol. Cryst. Liq. Cryst.*, **144**, 43 (1987).
11) T. Kitamura, A. Mukoh, M. Isogai, T. Inukai, K. Furukawa, and K. Terashima, *Mol. Cryst. Liq. Cryst.*, **136**, 167 (1986).
12) B. Otterholm, M. Nilsson, S. T. Lagerwall, and K. Skarp, *Liq. Cryst.*, **2**, 757 (1987).
13) A. Ezcurra, M. A. P. Jubindo, M. R. De La Fuente, J. Etxebarria, A. Remon, and M. J. Tello, *Liq. Cryst.*, **4**, 125 (1989).
14) T. Sakurai, N. Mikami, R. Higuchi, M. Honma, M. Ozaki, and K. Yoshino, *J. Chem. Soc., Chem. Commun.*, **1986**, 978.
15) J. W. Goodby, E. Chin, T. M. Leslie, J. M. Greary, and J. S. Patel, *J. Am. Chem. Soc.*, **108**, 4729 (1986).
16) K. Skarp and G. Andersson, *Ferroelectr., Lett. Sect.*, **6**, 67 (1986).
17) D. M. Walba, R. T. Vohra, N. A. Clark, M. A. Handschy, J. Xue, D. S. Parmar, S. T. Lagerwall, and K. Skarp, *J. Am. Chem. Soc.*, **108**, 7424 (1986).
18) Y. Haramoto and H. Kamogawa, *Chem. Lett.*, **1987**, 755.
19) T. Suzuki, T. Okawa, T. Ohnuma, and Y. Sakon, *Makromol. Chem., Rapid Commun.*, **9**, 755 (1988).
20) M. Dumon, H. T. Nguyen, M. Mauzac, C. Destrade, M. F. Achard, and H. Gasparoux, *Macromolecules*, **23**, 355 (1990).

21) S. Uchida, K. Morita, K. Miyoshi, K. Hashimoto, and K. Kawasaki, *Mol. Cryst. Liq. Cryst.*, **155**, 93 (1988).
22) V. P. Shibaev, M. V. Kozlovsky, N. A. Platé, L. A. Beresnev, and L. M. Blinov, *Liq. Cryst.*, **8**, 545 (1990).
23) K. Sugiyama and K. Shiraishi, *Makromol. Chem.*, **190**, 2381 (1989).
24) S. Bualek and R. Zentel, *Makromol. Chem.*, **189**, 797 (1988).
25) R. Zentel, G. Reckert, S. Bualek, and H. Kapitza, *Makromol. Chem.*, **190**, 2869 (1989).
26) S. Ujiie and K. Iimura, *Chem. Lett.*, **1990**, 1031.
27) J. Watanabe, A. Morita, M. Hayashi, and S. Kinoshita, *Polym. Prep. Jpn.*, **38**, 2371 (1989).
28) K. Shiraishi, K. Kato, and K. Sugiyama, *Chem. Lett.*, **1990**, 971.
29) K. Shiraishi, K. Kato, and K. Sugiyama, *Bull. Chem. Soc. Jpn.*, **63**, 1848 (1990).
30) K. Sugiyama, K. Kato, and K. Shiraishi, in contribution to *Chem. Lett.*
31) M. Portugall, H. Ringsdorf, and R. Zentel, *Makromol. Chem.*, **183**, 2311 (1982).
32) G. Smyth, S. K. Pollack, W. J. Macknight, and S. L. Hsu, *Liq. Cryst.*, **7**, 839 (1990).
33) A. Hallsby, M. Nilsson, and B. Otterholm, *Mol. Cryst. Liq. Cryst. Lett.*, **82**, 61 (1982).
34) K. Yoshino and M. Ozaki, *Jpn. J. Appl. Phys.*, **23**, L385 (1984).